

LETTER • OPEN ACCESS

## Biophysical permafrost map indicates ecosystem processes dominate permafrost stability in the Northern Hemisphere

To cite this article: Youhua Ran *et al* 2021 *Environ. Res. Lett.* **16** 095010

View the [article online](#) for updates and enhancements.

# ENVIRONMENTAL RESEARCH LETTERS



## OPEN ACCESS

RECEIVED  
23 March 2021

REVISED  
12 July 2021

ACCEPTED FOR PUBLICATION  
25 August 2021

PUBLISHED  
9 September 2021

Original content from this work may be used under the terms of the Creative Commons Attribution 4.0 licence.

Any further distribution of this work must maintain attribution to the author(s) and the title of the work, journal citation and DOI.



## LETTER

# Biophysical permafrost map indicates ecosystem processes dominate permafrost stability in the Northern Hemisphere

Youhua Ran<sup>1,5,\*</sup> M Torre Jorgenson<sup>2,\*</sup>, Xin Li<sup>3</sup>, Huijun Jin<sup>1,4</sup>, Tonghua Wu<sup>1,5</sup> Ren Li<sup>1,5</sup> and Guodong Cheng<sup>1,3</sup>

<sup>1</sup> Heihe Remote Sensing Experimental Research Station, Key Laboratory of Remote Sensing of Gansu Province, Northwest Institute of Eco-Environment and Resources, Chinese Academy of Sciences, Lanzhou 730000, People's Republic of China

<sup>2</sup> Alaska Ecosystems, Fairbanks, AK 99709, United States of America

<sup>3</sup> National Tibetan Plateau Data Center, State Key Laboratory of Tibetan Plateau Earth System, Resources and Environment, Institute of Tibetan Plateau Research, Chinese Academy of Sciences, Beijing 100101, People's Republic of China

<sup>4</sup> Institute of Cold-Regions Science and Engineering and School of Civil Engineering, Northeast Forestry University, Harbin 150040, People's Republic of China

<sup>5</sup> University of Chinese Academy of Sciences, Beijing 100049, People's Republic of China

\* Authors to whom any correspondence should be addressed.

E-mail: [ranyh@lzb.ac.cn](mailto:ranyh@lzb.ac.cn) and [ecoscience@alaska.net](mailto:ecoscience@alaska.net)

**Keywords:** permafrost, permafrost zonation map, biophysical, climate-driven, ecosystem-driven

## Abstract

The stability of permafrost is of fundamental importance to socio-economic well-being and ecological services, involving broad impacts to hydrological cycling, global budgets of greenhouse gases and infrastructure safety. This study presents a biophysical permafrost zonation map that uses a rule-based geographic information system (GIS) model integrating global climate and ecological datasets to classify and map permafrost regions (totaling  $19.76 \times 10^6 \text{ km}^2$ , excluding glaciers and lakes) in the Northern Hemisphere into five types: climate-driven (CD) (19% of area), CD/ecosystem-modified (41%), CD/ecosystem protected (3%), ecosystem-driven (29%), and ecosystem-protected (8%). Overall, 81% of the permafrost regions in the Northern Hemisphere are modified, driven, or protected by ecosystems, indicating the dominant role of ecosystems in permafrost stability in the Northern Hemisphere. Permafrost driven solely by climate occupies 19% of permafrost regions, mainly in High Arctic and high mountains areas, such as the Qinghai-Tibet Plateau. This highlights the importance of reducing ecosystem disturbances (natural and human activity) to help slow permafrost degradation and lower the related risks from a warming climate.

## 1. Introduction

Permafrost is defined as ground that continuously remains at or below 0 °C for at least 2 years. More than 99% of permafrost is distributed in the Northern Hemisphere (Obu *et al* 2019), with permafrost underlying approximately 25% of the land area (Zhang *et al* 2008). As a key component of the cryosphere in the Northern Hemisphere, the stability of permafrost is of fundamental importance to hydrological cycling, ecosystem processes, global budgets of major greenhouse gases, infrastructure security, and even public health (Immerzeel *et al* 2010, Lupascu *et al* 2014, Schuur *et al* 2015, McGuire *et al* 2018, Stella *et al* 2020), and thus are of importance to socio-economic and human well-being (Melvin *et al* 2017).

Observations show that permafrost is thawing around the world (Luo *et al* 2016, Biskaborn *et al* 2019, Ades *et al* 2020). The monitoring of mean annual ground temperature (MAGT) over the past few decades shows widespread permafrost warming at a rate of 0.14 °C–0.39 °C per decade (Biskaborn *et al* 2019). Active-layer thicknesses (ALTs) also are increasing, but with high spatial variability within a range of 0.15–1.95 cm yr<sup>-1</sup> (Ades *et al* 2020). Although permafrost is often viewed as a product of climate change, the large variations in permafrost properties and responses to a changing world are better understood as a result of complex interactions among biophysical factors, such as climate, vegetation, soil, and water (Shur and Jorgenson 2007). Changes in vegetation structure, soil organic matter,

and surface water during ecological succession and permafrost degradation create strong ecological feedbacks that can alter mean annual surface temperatures by as much as 10 °C–12 °C across local ecosystems (Jorgenson *et al* 2010, 2015). Some principles of non-zonal permafrost, even, have been applied to engineering in permafrost region (e.g. Cheng 2005). It still remains challenging to simulate the changes of permafrost at global scale, however, due to the lack of data and the model defects, whether physical-based model or statistical-based model. In practice, the prediction of the thermal state of permafrost is often controlled by climate (e.g. Chadburn *et al* 2017, Hjort *et al* 2018, Wang *et al* 2020). This may lead to underestimation of permafrost stability, with stability defined as a broad concept that includes both thermal and physical surface changes, because in very cold regions there can be substantial surface degradation (e.g. thermal erosion) even while deeper MAGT remain well below 0 °C and regions with ice-poor permafrost can thaw with little thaw settlement.

Instead, a biophysical classification of permafrost can form the basis for assessing permafrost vulnerability and the future risks to infrastructure and society from climate warming and natural and human disturbances, as well as their mitigative strategies and measures (Harris *et al* 2017, Ran *et al* 2018). The traditionally system based on areal continuity that classifies permafrost as continuous, discontinuous, sporadic, and isolated patches at global scale (Brown *et al* 1997) are useful for differentiating climatic influence, but do not explicitly recognize the role of ecosystem properties in formation and stability development of permafrost (Shur and Jorgenson 2007). Although a biophysical model and classification system have been developed to conceptualize the interactions and feedbacks of biophysical factors affecting the vulnerability of permafrost to climate change (Shur and Jorgenson 2007, Jorgenson *et al* 2010), at present there is no map at hemisphere scale that geographically partitions the climate and ecosystem interactions that affect the sensitivity of permafrost.

Here, we developed a rule-based decision framework to delineate the biophysical permafrost zones defined by Shur and Jorgenson (2007) in the Northern Hemisphere at 1 km resolution that incorporates the interactions among biophysical factors on permafrost stability. The extent of permafrost region is determined according to the probability of permafrost occurrence ( $>0$ ) derived from a machine-learning-based ensemble of simulation models that integrates unprecedentedly large amounts of ground measurement data (1002 boreholes) and multisource remote sensing data (Ran *et al* 2021). Then, we evaluated the ability of the new biophysical permafrost zonation to partition the variability of ALT, an important boundary layer between the atmosphere and permafrost that affects permafrost stability.

## 2. Materials and methods

### 2.1. Biophysical permafrost classification

Permafrost types defined by Shur and Jorgenson (2007) were used to describe the complex interactions of climatic and ecological processes. The system classifies the permafrost into five types: climate-driven (CD), climate-driven/ecosystem-modified (CDEM), CDEM, ecosystem-driven (ED), and ecosystem-protected (EP). The definition of the biophysical zonation of permafrost can be found in table 1.

### 2.2. Simulation of permafrost extent

The extent of the permafrost region for 2000–2016 in the Northern Hemisphere at 1 km resolution was derived from the probability of permafrost occurrence ( $>0$ ) that was calculated as the fraction of 1000 ensemble model runs with MAGT below 0 °C. The MAGT was simulated using four statistical learning techniques, including a generalized additive model, support vector regression, random forest, and extreme gradient boosting by integrating the unprecedented amounts of ground measurement of MAGT (i.e. 1002 boreholes) and the remotely sensed freezing degree-days, thawing degree-days (TDDs), leaf area index, snow cover duration, precipitation, solar radiation, soil organic content (SOC), bulk density, and coarse fragments content (more details can be found in Ran *et al* 2021). As a boundary, the simulated permafrost extent excluding glaciers and lakes was used to control the zonation extent in the next section.

### 2.3. Decision making process of biophysical permafrost zonation

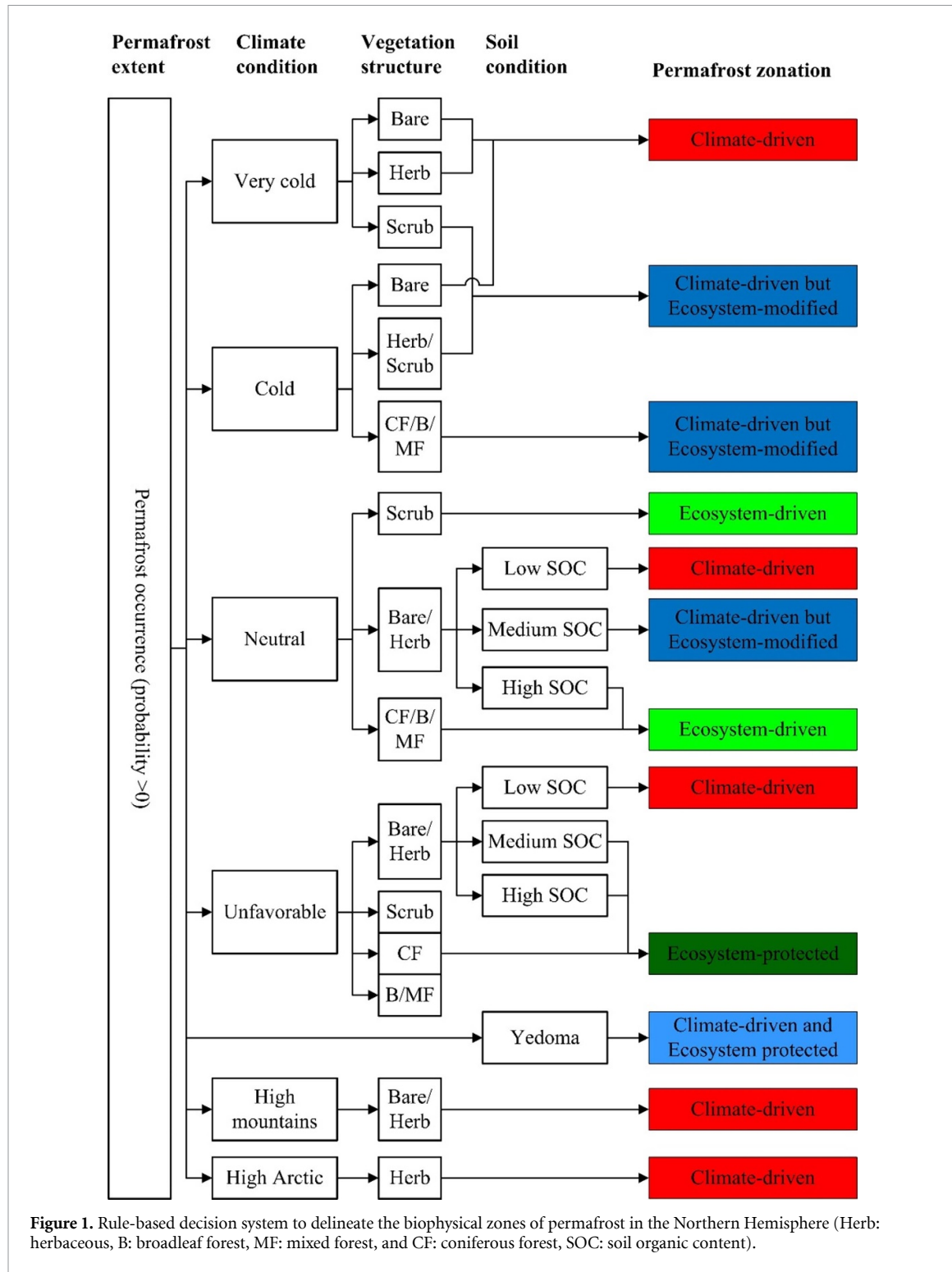
A rule-based GIS approach was used to delineate the permafrost zonation based on permafrost extent, climate conditions, vegetation structure, soil conditions, and topographic conditions, as well as a specific map of extremely ice-rich Pleistocene permafrost (Yedoma) (figure 1). While these global datasets do not capture the complexity of ecological successional patterns and processes across diverse ecoregions, these structural inputs served as surrogates for partitioning the formative biophysical factors that drive permafrost zonation. Following Shur and Jorgenson (2007), climate conditions were classified into four levels that include very cold ( $\leq -16$  °C mean annual air temperatures, MAAT), cold ( $-16$  °C to  $-7$  °C), neutral ( $-7$  °C to  $-2$  °C, conditions where either permafrost aggradation or degradation can occur), and unfavorable ( $\geq -2$  °C) based on MAAT of Worldclim 2.1, a spatially downscaled and bias-corrected climate data with 1 km resolution for 1970–2000 (Fick and Hijmans 2017). These temperature cutpoints are consistent with the permafrost zonation boundaries on Brown *et al* (1997). For vegetation structure, the most frequent land cover during 2000–2015 sourced from European Space Agency Climate Change Initiative

**Table 1.** The definition of the biophysical zonation of permafrost (according to Shur and Jorgenson 2007).

Permafrost type	Formation conditions	Vulnerability
Climate-driven (CD)	Permafrost in cold or very cold climate conditions where permafrost forms independent of vegetation and immediately after the surface is exposed to the atmosphere and even under shallow water.	This permafrost is the most vulnerable type to rapid climate warming because the active layer is already near maximum for regional conditions. It is also slow to stabilize or recover because vegetation and soil development is very slow.
Climate-driven/ ecosystem-modified (CDEM)	Permafrost in cold areas formed as CD, but ground ice and thermal regimes are modified by vegetation succession and organic-matter accumulation.	It is more thermally stable, but less thaw stable (more ice-rich), than CD permafrost. This type of permafrost can persist for a long time as EP during warming climates.
Climate-driven/ ecosystem-protected (CDEP)	Permafrost was formed under a very cold climate, such as during the Late Pleistocene or the Little Ice Age, and has unique cryostructures that persist under a neutral climate protected by the ecosystems in the late-successional stage. Related principally to Yedoma and buried glacial ice.	Removal of vegetation and organic soil by natural or human disturbances typically leads to permafrost degradation, and once degraded the original permafrost characteristics cannot be re-established. The degraded portion of the upper soil profile, however, can recover as ED permafrost in some situations.
Ecosystem-driven (ED)	Permafrost was formed in poorly drained, low-lying or north-facing landscape conditions where climate alone is insufficient to cause permafrost formation, and thus strongly influenced by vegetation succession and organic-matter accumulation.	This permafrost thaws slowly from the surface once disturbed by fire or human activity. It can partially or totally degrade at depth. Degradation continues until vegetation recovery creates conditions at which the mean annual temperature at the bottom of the active layer becomes $<0$ °C.
Ecosystem-protected (EP)	Permafrost can persist under late-successional stages of ecosystem development, but cannot be reformed after disturbance.	Permafrost persists as sporadic patches under warmer climates, but cannot be re-established after disturbance. It is the most sensitive type to ecosystem damage.

program was grouped into five classes: bare, herbaceous, scrub, broadleaf/mixed, and coniferous. The vegetation structure was used because it alters the microclimate and snow regimes: low structure has little effect while coniferous structure reduces summer radiation-driven soil heat input and winter snow cover driven soil heat loss. We assumed herbaceous structure has little effect on thermal regimes in High Arctic regions where the herbaceous land cover was treated as bare. High Arctic terrestrial boundaries were defined by the Circumpolar Arctic Vegetation Mapping Project ([www.geobotany.uaf.edu/cavm/](http://www.geobotany.uaf.edu/cavm/)). To resolve a few mismatches between the global datasets of climate and vegetation, we assigned forests under cold climates (rarely occurs) to CDEM permafrost. For soil condition, SOC from SoilGrids250 was classified as three levels: low ( $\leq 20$  g kg $^{-1}$ ), medium (20–200 g kg $^{-1}$ ), and high ( $>200$  g kg $^{-1}$ ) (Hengl *et al* 2017). To resolve mismatches between climate and vegetation in permafrost distribution in neutral and unfavorable conditions, SOC was used to help differentiate CD permafrost associated bare vegetation and CDEM permafrost associated with herb vegetation (assuming organic accumulation helps

modified active layer and ground ice responses). Further, high SOC was used to differentiate EP permafrost along the southern permafrost margin with climate unfavorable to permafrost formation. Third, CDEP permafrost is a relic of the extremely cold temperatures during the Pleistocene, and cannot form under current climates. Thus, the Yedoma distribution sourced from Database of Ice-Rich Yedoma permafrost (Strauss *et al* 2016) was assigned as CDEP permafrost. While Yedoma exists across a wide range of temperature conditions from the southern limit of permafrost to the High Arctic, we considered it all to be CDEP permafrost because it has persisted in places for tens of thousands of years by ecological conditions at the surface across all climates (Shur and Jorgenson 2007). In high mountain areas, except where Yedoma was mapped, the bare and herbaceous vegetation classes were assigned as CD permafrost where the vegetation structure is insufficient to develop ecosystem-modified or EP permafrost. The high mountains extent was defined based on slope ( $\geq 51\%$ ) and relative relief ( $>900$  m) (Karagulle *et al* 2017). Finally, the ArcGIS majority statistics process with a rectangular 5 × 5 neighborhood was used to



remove the small inclusions and non-permafrost area was masked using the permafrost extent layer mentioned in last section.

## 2.4. Statistical analysis

T-test was used to perform the correlation test of ALT with TDDs. Student–Newman–Keuls test was used to perform the test of statistically difference of correlation among five biophysical permafrost zones: CD, CDEM, CDEP, ED, and EP. The SPSS® statistics software (v20) is used to implement this test.

### 3. Results and discussion

### 3.1. Biophysical permafrost zonation map

The modeled map shows that 19% ( $3.66 \times 10^6 \text{ km}^2$ ) of permafrost regions is solely CD, mostly found in the Canadian High Arctic (Canadian Archipelago) and high mountains areas, primarily on the Qinghai-Tibet Plateau (figure 2). This type is highly vulnerable to both rapid climate warming and disturbance (at least ice wedges), because the ALT is already near its maximum for regional conditions

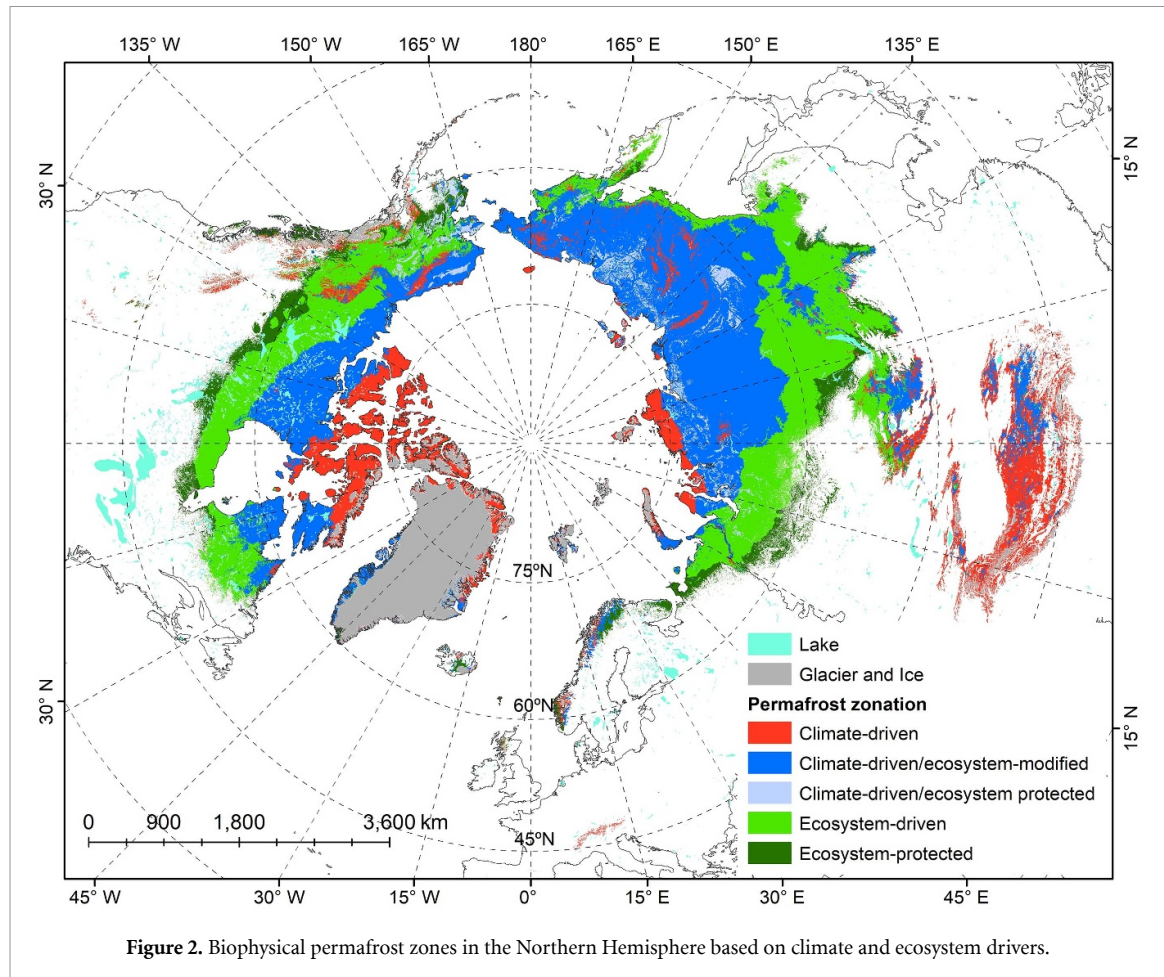


Figure 2. Biophysical permafrost zones in the Northern Hemisphere based on climate and ecosystem drivers.

(Shur and Jorgenson 2007, Farquharson *et al* 2019, Ward Jones *et al* 2019). However, recovery towards original permafrost characteristics is unlikely or very slow because vegetation little effect on soil properties and organic-matter accumulation. Thus, the amplified warming in western Qinghai–Tibet Plateau or High Arctic and associated thermokarst development may be the main challenge to the permafrost stability of these areas in the future.

Both climate and ecosystems are strong drivers in 44% ( $8.68 \times 10^6 \text{ km}^2$ ) of permafrost regions, with 41% being CDEM and 3% being CDEP. The CDEM permafrost is mainly distributed across northern Eurasia and northern part of North America, as well as the Southern Mongolia and eastern Tibetan plateaus. This type is initially formed as CD, but its ground temperatures and active-layer properties are later modified by changes in vegetation structure and soil organic-matter accumulation during ecological succession (Jorgenson *et al* 2015). These successional changes are fundamental to the development of an ice-rich intermediate layer at the top of permafrost (Shur *et al* 2005). It is more thermally stable, but less than stable due to aggrading ground ice, than the original CD permafrost. In most situations, permafrost degradation affects only the top few meters of the ground surface. Thus, climate

warming and ecosystem disturbances are the main factors affecting permafrost stability in this zone, including the eastern Qinghai–Tibet Plateau where infrastructure development is most prevalent (Jin *et al* 2008). The map of CDEM permafrost is consistent with field (Jorgenson and Shur 2007, Bockheim and Hinkel 2012) and remote sensing (Jones *et al* 2015, Farquharson *et al* 2016, Nitze *et al* 2018, Lu *et al* 2020) that show disturbance, thermokarst, and ecological surface conditions interact to strongly influence ground-ice dynamics and permafrost stability.

CDEP permafrost is a special class that formed under much colder climatic conditions and could not be modeled using datasets of contemporary climate. It mainly pertains to extremely ice-rich silt deposits formed in the Pleistocene, termed Yedoma (Strauss *et al* 2017), Late Pleistocene glacial deposits (Kokelj *et al* 2017), and ice-wedge terrain in neutral ( $-7^\circ \text{C}$  to  $-2^\circ \text{C}$ ) climate (Froese *et al* 2008). It has persisted for thousands to hundreds of thousands of years because of ecosystem (vegetation and peat) protection (Froese *et al* 2008). Removal of vegetation and organic soil by wildfires, geomorphic processes (e.g. fluvial-lacustrine erosions, hillslope thaw slumps), or human disturbances, typically leads to permafrost degradation, and once permafrost is degraded, the original permafrost features cannot be re-established

(Shur *et al* 2021). The degraded portion of the upper soil profile, however, can recover as ED permafrost in situations where the rates of ecological succession and recovery of downward ground freezing are more rapid than the rate of deep thawing, as this reworked surface layer is integral to the persistence of Yedoma (Kanevskiy *et al* 2014).

The remaining 37% ( $7.42 \times 10^6 \text{ km}^2$ ) of permafrost regions is either ED (29%) or EP (8%). The ED permafrost occurs mainly along the southern margins of discontinuous permafrost zones across Eurasia and North America. Across this region, discontinuous permafrost and unfrozen ground patches occur in close proximity under the same climate, and is primarily associated with late-successional ecosystems with well developed, thick soil organic layers. Once disturbed by fires, human activities, or extreme climate events, it can either degrade slowly from downward thawing from the ground surface or rapidly through lateral thaw along the margins of thermokarst lakes, rivers, bogs, and fens. Depending on the rate of permafrost thawing, amount of thaw settlement, and rate of ecological recovery, permafrost can be thawed completely to the underlying unfrozen ground, or can be re-established over time through ecological successions (Jorgenson *et al* 2013). In contrast, EP permafrost is distributed as sporadic patches along the southern margin of the permafrost zones and can persist in areas with MAAT as warm as  $2^\circ\text{C}$  (French 2008, Jones *et al* 2016). It is limited to late-successional ecosystems, thus, it is the permafrost type most sensitive to disturbances and cannot be re-established after disturbances under the current climate (Jorgenson and Shur 2007). The distribution of these two types on our map are difficult to validate through remote sensing because they frequently occur in patches much smaller than our map scale, both frozen and unfrozen ground can occur under late successional ecosystems, and both permafrost types can be associated with late successional ecosystems (e.g. black spruce needleleaf forests, tussock scrub bogs) that cannot be differentiated with the global vegetation classes.

### 3.2. Uncertainty of permafrost zonation

The permafrost extent of the biophysical model is similar to the map of circumpolar permafrost zones by Brown *et al* (1997) based on regional mapping and field expertise, and the recent northern hemisphere map by Obu *et al* (2019) based on a thermal modeling. Both of them have divided permafrost zones mainly on its areal continuity (e.g. continuous versus discontinuous). The total area of permafrost extent in our map is  $19.76 \times 10^6 \text{ km}^2$  (excluding glaciers and lakes), compared to  $22.8 \times 10^6 \text{ km}^2$  in that of the Brown *et al* (1997) and  $20.8 \times 10^6 \text{ km}^2$  in that of the Obu *et al* (2019). When evaluating the sensitivity of the biophysical model by varying temperature thresholds by  $\pm 1^\circ\text{C}$ , permafrost extent varied

little for CD permafrost ( $3.73\text{--}3.64 \times 10^6 \text{ km}^2$ ), but was higher for CDEM ( $8.89\text{--}7.2 \times 10^6 \text{ km}^2$ ). Furthermore, there is addition uncertainty due to the broad mismatch of boreal forest distribution across a range of MAAT ( $-5^\circ\text{C}$  to  $-9^\circ\text{C}$ ), with our model using an intermediate value ( $-7^\circ\text{C}$ ). Extent of CDEP permafrost ( $0.61\text{--}0.62 \times 10^6 \text{ km}^2$ ) did not vary in the model because it was based solely on the map of Yedoma distribution. ED permafrost ( $5.81\text{--}5.4 \times 10^6 \text{ km}^2$ ) was relatively insensitive to the lower temperature threshold, while EP permafrost ( $0.72\text{--}2.9 \times 10^6 \text{ km}^2$ ) was highly sensitive presumably because small temperature variations occur over broad areas at the southern margin and the inadequacy of the coniferous structure to represent late-successional vegetation-soil relationships in complex boreal landscapes. The temperature thresholds, as well as the other rules, lead to regional differences among Russia, Canada, China, and Alaska that are somewhat inconsistent with our regional knowledge, but could not be resolved through universal rules.

### 3.3. Application of biophysical permafrost zonation: variability of ALT

Biophysical zonation of permafrost is fundamental for understanding the heterogeneous responses of permafrost to climate change and to natural and human disturbances. While climate is the fundamental controller for permafrost distribution at a global scale, ecosystem properties strongly affect variations in permafrost distribution and hydrothermal dynamics of permafrost at local to landscape scales. Overall, in 62% ( $12.34 \times 10^6 \text{ km}^2$ ) of the permafrost regions in the Northern Hemisphere, permafrost is driven by climate, although part of it can be modified or protected by ecosystems, i.e. permafrost is formed regardless of ecological boundary conditions. In contrast, the role of ecosystems in driving, modifying, or protecting permafrost is important in 81% ( $16.1 \times 10^6 \text{ km}^2$ ) of the permafrost regions in the Northern Hemisphere. These results indicate that the most important short-term strategy for mitigating potential ground instability due to thawing permafrost and for reducing the related risks, such as the permafrost greenhouse gases climate feedback at global scale, may be to minimize the disturbances to the ecosystem in permafrost regions. For examples, disturbance such as wildfires, thermokarst development, grazing, and construction, have been found as a trigger factors influencing the carbon balance (Mu *et al* 2020) in permafrost regions, even in high Arctic tundra ecosystem (Cassidy *et al* 2016). This finding also highlights the importance of incorporating ecosystem disturbance processes into physical-based and statistical models to lower the uncertainty of permafrost projections.

In one application of the new map, we assessed its ability to partition the variability of ALT, an important boundary or buffer between the

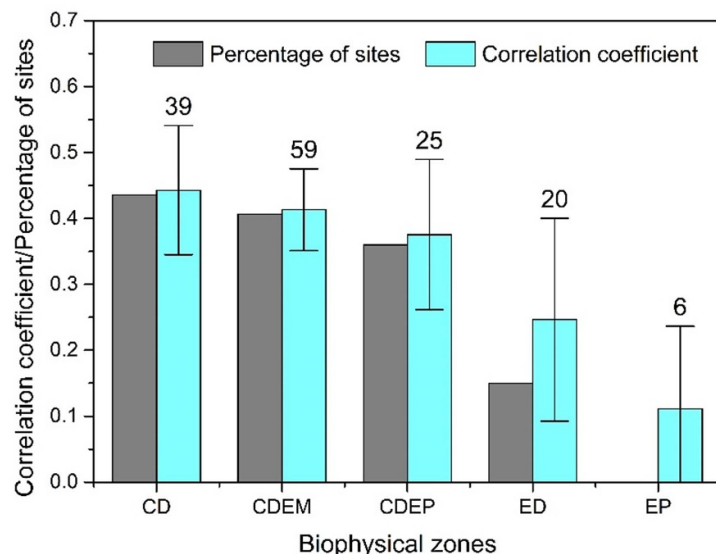


**Figure 3.** The percentage of sites with significant ( $p < 0.05$ ) correlations (gray bars) of ALT with TDDs from 1996 to 2018, and the mean of correlation coefficients ( $\pm 95\%$  CI, blue bars) among five biophysical permafrost zones: climate-driven (CD), climate-driven/ecosystem-modified (CDEM), climate-driven/ecosystem-protected (CDEP), ecosystem-driven (ED), and ecosystem-protected (EP). The number above each bar is the sample size.

atmosphere and permafrost. We correlated ALT measurements at 149 sites from the International Permafrost Association Global Terrestrial Network for Permafrost (Biskaborn *et al* 2019) and some unpublished data with a nearly complete time-series ( $\geq 8$  years of data per site) with TDDs (annual sum of degree-days above  $0^{\circ}\text{C}$ ) derived from the spatially downscaled historical monthly weather reanalysis product of Worldclim 2.1 with 2.5 min spatial resolution (<http://worldclim.org>) from 1996 to 2018. The strength of the correlation coefficient of ALT with TDD varied significantly ( $p < 0.05$ ) among CD and ecosystem driven or protected permafrost zones, with the best correlation for the CD permafrost and the worst correlation for the EP permafrost (figure 3). The correlation decreased linearly ( $p < 0.01$ ) from the CD to the EP permafrost types, indicating that climate is the primary driver at high latitudes and that at lower latitudes, ecosystem characteristics replace the climate as the primary driver for permafrost boundary conditions (surface offset and thermal offset). This zonation also is likely to be useful for partitioning the variability of other important permafrost features, such as permafrost temperatures, ground-ice content, and thermokarst modes, and for analyzing infrastructure risks.

#### 4. Conclusions

This study presents a biophysical permafrost zonation map that uses a new rule-based GIS model integrating global climate and ecological characteristics to classify and map permafrost regions in the Northern Hemisphere (totaling  $19.76 \times 10^6 \text{ km}^2$  excluding glaciers and lakes) into five types: CD (19%), CDEM

(41%), CDEP (3%), ED (29%), and EP (8%). Overall, 81% of the permafrost regions in the Northern Hemisphere are affected by ecosystems, indicating the dominant role that ecological processes have in controlling permafrost stability. The finding highlights the importance of reducing ecosystem disturbances (natural and human activity) to help slow permafrost degradation and lower the related risks from a warming climate. In evaluating the ability of the new map to partition the variability of ALT, an atmosphere-soil boundary layer important to permafrost stability, the strength of climate-ALT relationships was higher in regions with climate-driven permafrost and lower for ecosystem-driven and -protected permafrost, indicating that ecological properties dominate permafrost stability in these areas. The map also is potentially useful for predicting permafrost degradation and ecological transitions, and for assessing the future risks to infrastructure and society from climate warming, as well as their mitigative strategies and measures.

#### Data availability statement

The biophysical permafrost zonation map generated by the study are publicly available and can be downloaded via <https://doi.org/10.11888/Geocry.tpdc.271659>. Other data are available from the authors on reasonable request.

The data that support the findings of this study are available upon reasonable request from the authors.

#### Acknowledgments

This study was jointly supported by the Strategic Priority Research Program of the Chinese Academy of

Sciences (Grant Number XDA19070204), National Natural Science Foundation of China projects (Grant Number 41471359), and US National Science Foundation (Grant OPP-1820883).

## Conflict of interest

The authors declare no competing interests.

## ORCID iDs

Youhua Ran  <https://orcid.org/0000-0001-7774-4612>

Tonghua Wu  <https://orcid.org/0000-0002-5084-3570>

## References

Ades M *et al* 2020 Global climate [in 'State of the Climate in 2019'] *Bull. Am. Meteorol. Soc.* **101** S9–127

Biskaborn B K *et al* 2019 Permafrost is warming at a global scale *Nat. Commun.* **10** 1–11

Bockheim J G and Hinkel K M 2012 Accumulation of excess ground ice in an age sequence of drained thermokarst lake basins, Arctic Alaska *Permafrost. Periglac. Process.* **23** 231–6

Brown J, Ferrians O J, Heginbottom J A and Melnikov E S 1997 Circum-Arctic map of permafrost and ground ice conditions *US Geological Survey* (Reston, VA) pp CP–45

Cassidy A E, Christen A and Henry G H R 2016 The effect of a permafrost disturbance on growing-season carbon-dioxide fluxes in a high Arctic tundra ecosystem *Biogeosciences* **13** 2291–303

Chadburn S E, Burke E J, Cox P M, Friedlingstein P, Hugelius G and Westermann S 2017 An observation-based constraint on permafrost loss as a function of global warming *Nat. Clim. Change* **7** 340–4

Cheng G 2005 A roadbed cooling approach for the construction of Qinghai–Tibet Railway *Cold Reg. Sci. & Technol.* **42** 169–76

Farquharson L M, Mann D H, Grosse G, Jones B M and Romanovsky V E 2016 Spatial distribution of thermokarst terrain in Arctic Alaska *Geomorphology* **273** 116–33

Farquharson L M, Romanovsky V E, Cable W L, Walker D A, Kokelj S V and Nicolsky D 2019 Climate change drives widespread and rapid thermokarst development in very cold permafrost in the Canadian High Arctic *Geophys. Res. Lett.* **46** 6681–9

Fick S E and Hijmans R J 2017 WorldClim 2: new 1-km spatial resolution climate surfaces for global land areas *Int. J. Climatol.* **37** 4302–15

French H 2008 Recent contributions to the study of past permafrost *Permafrost. Periglac. Process.* **19** 179–94

Froese D G, Westgate J A, Reyes A V, Enkin R J and Preece S J 2008 Ancient permafrost and a future, warmer arctic *Science* **321** 1648

Harris S A, Bouchkov A and Cheng G D 2017 *Geocryology: Characteristics and Use of Frozen Ground and Permafrost Landforms* (Boca Raton, FL: CRC Press)

Hengl T *et al* 2017 SoilGrids250m: global gridded soil information based on machine learning *PLoS One* **12** e0169748

Hjort J, Karjalainen O, Aalto J, Westermann S, Romanovsky V E, Nelson F E, Etzelmüller B and Luoto M 2018 Degrading permafrost puts Arctic infrastructure at risk by mid-century *Nat. Commun.* **9** 5147

Immerzeel W W, van Beek L P and Bierkens M F 2010 Climate change will affect the Asian water towers *Science* **328** 1382–5

Jin H-J, Yu Q-H, Wang S-L and Lü L-Z 2008 Changes in permafrost environments along the Qinghai–Tibet engineering corridor induced by anthropogenic activities and climate warming *Cold Reg. Sci. & Technol.* **53** 317–33

Jones B M, Baughman C A, Romanovsky V E, Parsekian A D, Babcock E L, Stephani E, Jones M C, Grosse G and Berg E E 2016 Presence of rapidly degrading permafrost plateaus in south-central Alaska *Cryosphere* **10** 2673–92

Jones B M, Grosse G, Arp C D, Miller E, Liu L, Hayes D J and Larsen C 2015 Recent arctic tundra fire initiates widespread thermokarst development *Sci. Rep.* **5** 15865

Jorgenson M T *et al* 2013 Reorganization of vegetation, hydrology and soil carbon after permafrost degradation across heterogeneous boreal landscapes *Environ. Res. Lett.* **8** 035017

Jorgenson M T, Kanevskiy M Z, Shur Y, Moskalenko N, Brown D R, Wickland K, Striegl R and Koch J 2015 Role of ground-ice dynamics and ecological feedbacks in recent ice-wedge degradation and stabilization *J. Geophys. Res.* **120** 2280–97

Jorgenson M T, Romanovsky V, Harden J, Shur Y, O'Donnell J, Schuur E A G, Kanevskiy M and Marchenko S 2010 Resilience and vulnerability of permafrost to climate change *Can. J. For. Res.* **40** 1219–36

Jorgenson M T and Shur Y 2007 Evolution of lakes and basins in northern Alaska and discussion of the thaw lake cycle *J. Geophys. Res.* **112** F02S17

Kanevskiy M Z, Jorgenson M T, Shur Y, O'Donnell J A, Harden J W, Zhuang Q L and Fortier D 2014 Cryostratigraphy and permafrost evolution in the lacustrine lowlands of West-Central Alaska *Permafrost. Periglac. Process.* **25** 14–34

Karagulle D, Frye C, Sayre R, Breyer S, Aniello P, Vaughan R and Wright D 2017 Modeling global Hammond landform regions from 250-m elevation data *Trans. GIS* **21** 1040–60

Kokelj S V, Lantz T C, Tunnicliffe J, Segal R and Lacelle D 2017 Climate-driven thaw of permafrost preserved glacial landscapes, northwestern Canada *Geology* **45** 371–4

Lu P, Han J, Li Z, Xu R, Li R, Hao T and Qiao G 2020 Lake outburst accelerated permafrost degradation on Qinghai–Tibet Plateau *Remote Sens. Environ.* **249** 112011

Luo D, Wu Q, Jin H, Marchenko S S, Lu L Z and Gao S R 2016 Recent changes in the active layer thickness across the northern hemisphere *Environ. Earth Sci.* **75** 555

Lupascu M, Welker J M, Seibt U, Maseyk K, Xu X and Czimczik C I 2014 High Arctic wetting reduces permafrost carbon feedbacks to climate warming *Nat. Clim. Change* **4** 51–55

McGuire A D *et al* 2018 Dependence of the evolution of carbon dynamics in the northern permafrost region on the trajectory of climate change *Proc. Natl Acad. Sci. USA* **115** 3882–7

Melvin A M *et al* 2017 Climate change damages to Alaska public infrastructure and the economics of proactive adaptation *Proc. Natl Acad. Sci. USA* **114** E122–31

Mu C *et al* 2020 The status and stability of permafrost carbon on the Tibetan Plateau *Earth Sci. Rev.* **211** 103433

Nitze I, Grosse G, Jones B M, Romanovsky V E and Boike J 2018 Remote sensing quantifies widespread abundance of permafrost region disturbances across the Arctic and Subarctic *Nat. Commun.* **9** 5423

Obu J *et al* 2019 Northern Hemisphere permafrost map based on TTOP modelling for 2000–2016 at 1 km<sup>2</sup> scale *Earth Sci. Rev.* **193** 299–316

Ran Y *et al* 2021 New high-resolution estimates of the permafrost thermal state and hydrothermal conditions over the Northern Hemisphere *Earth Syst. Sci. Data Discuss.* 1–27

Ran Y, Li X and Cheng G 2018 Climate warming over the past half century has led to thermal degradation of permafrost on the Qinghai–Tibet Plateau *Cryosphere* **12** 595–608

Schuur E A G *et al* 2015 Climate change and the permafrost carbon feedback *Nature* **520** 171–9

Shur Y L and Jorgenson M T 2007 Patterns of permafrost formation and degradation in relation to climate and ecosystems *Permafro. Periglac. Process.* **18** 7–19

Shur Y, Hinkel K M and Nelson F E 2005 The transient layer: implications for geocryology and climate-change science *Permafro. Periglac. Process.* **16** 5–17

Shur Y, Jones B M, Kanevskiy M, Jorgenson T, Jones M K, Fortier D, Stephani E and Vasiliev A 2021 Fluvio-thermal erosion and thermal denudation in the yedoma region of northern Alaska: Revisiting the Itkillik River exposure *Permafrost and Periglac Process* **32** 277–98

Stella E, Mari L, Gabrieli J, Barbante C and Bertuzzo E 2020 Permafrost dynamics and the risk of anthrax transmission: a modelling study *Sci. Rep.* **10** 1–12

Strauss J *et al* 2016 Database of Ice-Rich Yedoma permafrost (IRYP) PANGAEA (<https://doi.org/10.1594/PANGAEA.861733>)

Strauss J *et al* 2017 Deep Yedoma permafrost: a synthesis of depositional characteristics and carbon vulnerability *Earth Sci. Rev.* **172** 75–86

Wang T, Yang D, Yang Y, Piao S, Li X, Cheng G and Fu B 2020 Permafrost thawing puts the frozen carbon at risk over the Tibetan Plateau *Sci. Adv.* **6** eaaz3513

Ward Jones M K, Pollard W H and Jones B M 2019 Rapid initialization of retrogressive thaw slumps in the Canadian high Arctic and their response to climate and terrain factors *Environ. Res. Lett.* **14** 055006

Zhang T, Barry R G, Knowles K, Heginbottom J A and Brown J 2008 Statistics and characteristics of permafrost and ground-ice distribution in the Northern Hemisphere *Polar Geogr.* **31** 47–68